The Crystal Structure and Genesis of the Gold Telluride Minerals

Departmental Undergraduate Thesis

Matthew DeWayne Dye

Department of Geological Sciences,

University of Colorado

March, 2011

Committee Members:

Dr. Joseph R. Smyth

Dr. William W. Atkinson, Jr.

Dr. Bruce A. Geller

Table of Contents

List of Figures Page Number

Abstract

The primary gold telluride minerals are represented by three distinct species: calaverite ($Au_{0.85}Ag_{0.15}Te_2$), krennerite ($Au_{0.75}Ag_{0.25}Te_2$), and sylvanite ($AuAgTe_4$). All three of these mineral species are historically important ores of gold (and to a lesser extent silver), and are found in relative abundance within several of the world's major telluride districts. Detailed studies on the atomic structure of the gold telluride minerals began in 1935 with work on calaverite. Additional research on krennerite and sylvanite was conducted in the following years. The mineral class was then revisited in 1984, yielding several redeterminations of crystal structure. Through technological advancements in both analytical technique and structure refinement algorithms, the author sought to again revisit the determination of crystal structure in an attempt to both verify the results of previous investigations, and to attempt to better resolve the atomic structure parameters in the literature.

In the course of this research, several structure determinations were performed on euhedral sub-millimeter crystals of calaverite, krennerite, and sylvanite that were harvested from specimens within the University of Colorado's mineral collection. Structurally, krennerite is the most ordered of these three species. Single crystal structural studies yielded several datasets, including a refinement of the krennerite structure with a reliability factor of 0.024- a significantly lower value than was attained in any of the previous studies. Atomic position coordinates derived from this dataset were resolved to a precision of nearly one order of magnitude over that of previous work.

In addition to the primary structural studies, research into both crystal chemistry and paragenesis were performed using the specimen which provided the krennerite refinement discussed above. These latter studies provided information as to the specific crystal chemistries of the ore minerals found in the specimen, and also allowed for the determination of the mineralizing sequence of the hydrothermal fluids responsible for producing the krennerite used in the structural refinement. By combining the data derived in the structural study with observations made during these studies, a more coherent picture of the mineralizing system has emerged.

Other original work contained in this thesis include the redetermination of the calaverite unit cell, as well as reanalysis of the crystal chemistry of an indeterminate gold telluride phase that contains silver concentrations which lie between the accepted values for either calaverite or krennerite.

Introduction:

The gold tellurides represent a unique class of minerals wherein elemental gold is atomically bound to elemental tellurium, producing one of the few known naturally occurring instances of a stochiometric solid of gold and an additional element. Other examples of atomically bound gold minerals include aurostibite ($AuSb_2$) which is found in sulfur deficient portions of gold systems rich in antimony minerals, Maldonite (Au_2Bi), which is found in high temperature gold systems rich in bismuth, auricupride ($CuAu_3$), which results from the low temperature un-mixing of gold and copper alloys, and Fischesserite (Ag_3AuSe_2), which is a selenium analog to petzite (AuAg3Te4). Although occurrences of these minerals are known, none has the widespread occurrence seen in the gold tellurides. Within the gold telluride class of minerals, silver commonly substitutes for some fraction of the gold, leading to the variable crystal chemistry and atomic structure of the three primary species as described in later sections. Accordingly, the primary gold (silver) tellurides constitute an historically important ore of both gold and silver, with occurrences noted in such world-class mining districts as the Cripple Creek and Boulder County Mining Districts of Colorado, the Baia de Aries (Offenbánya) and Nagyág (Sacarîmb) regions of Romania, the Emperor Mine in Vatukoula, Fiji, and the Goldfields-Esperance Region in Kalgoorlie, Australia (Cabri, 1965; Geller, 1993).

Despite their well-known occurrence within these and other major districts, the gold telluride minerals are quite rare. This is largely due to the scarcity of tellurium within the earth's crust, which is thought to only comprise an average of about 1 ppb of mafic, intermediate, and felsic igneous rocks (Geller, 1993). Significant occurrences of gold telluride minerals are found in both high-level epithermal vein systems, as well as in orogenic (mesothermal) deposits. Examples of the former include the Gold Hill, Sunshine, and Jamestown Mining Districts of Boulder County, Colorado. Examples of the latter include the Angel's Camp District in the Mother Lode Belt of California, as well as the Kirkland-Larder Mining District in Ontario, Canada.

Within high-level epithermal vein systems, the source of the tellurium component is thought to be primarily from silica undersaturated to oversaturated alkaline mineralizing intrusions (Geller, 1993; Saunders, 1986). These intrusions may be exposed at the surface through erosion, or may exist as blind porphyries at depth. For example, the presence of a blind porphyry to the northwest of the Magnolia Mining District in Boulder County was hypothesized by Geller (1993) using residual gravity data.

History:

Despite their academic interest and economic importance, very little information on the history of the gold telluride minerals is available in the literature. Accordingly, only a brief synopsis is provided here. Calaverite was first discovered in Calaveras County, CA in 1861 at the Stanislaus Mine (type locality), Carson Hill, Angels Camp District. The mineral was named for the county in 1868. Krennerite was discovered in 1877 as a constituent of the telluride ores from the Sacarîmb region of Romania. It was first described by József Sándor Krenner (3 March 1839- 6 January 1920), and was later named in his honor. Sylvanite was also discovered in Romania, in the Baia de Aries (Offenbánya) region of Transylvania. It was first described in 1796, and was later named after the Transylvania region.

Crystal Chemistry and Structure:

The primary gold (silver) telluride minerals are represented by three distinct species: calaverite ($Au_{0.85}Ag_{0.15}Te_2$), krennerite ($Au_{0.75}Ag_{0.25}Te_2$), and sylvanite ($AuAgTe_4$). All three of these minerals are chemically distinguished by different levels of silver substitution. Based on synthesis studies, calaverite has a stable compositional range of 0.0 to 2.8 wt% Ag, krennerite 3.4 to 6.2 wt % Ag, and sylvanite 6.7 to 13.23 wt % Ag (Cabri, 1965). Whereas calaverite and sylvanite both have a centric monoclinic structure, krennerite is distinctively acentric orthorhombic. Calaverite has space group *C 2/m*, krennerite has space group *Pma2*, and sylvanite has space group *P 2/c*. Despite this difference in crystal system and space group, sylvanite and krennerite share striking similarities in their internal structure.

The structure of calaverite was first determined by Tunnell and Ksanda in 1935. This same group then determined the crystal structure of krennerite in 1936, and that of sylvanite in 1937 (Tunnell, 1954). Further detailed investigations on the atomic arrangements of calaverite, sylvanite, and krennerite were published by Tunnell (et. al) in 1936, 1941, and 1950, respectively. Later refinements of these structures were carried out by Franz Pertlik (1984a; 1984b; 1984c).

Krennerite is one of two gold ditelluride members of the kostovite-calaverite series (Strunz classification II/D.16). Sylvanite is also part of this series, but is classified as a gold-silver telluride. Each of these species inherently includes some small quantity of silver, with variable amounts present as described above. Therefore, the chemical formula for each of the two gold ditelluride members may be written as $Au_{1-x}Ag_xTe_2$ (Pertlik, 1984b). Volumetrically, sylvanite represents a doubling of the calaverite cell commensurate with the incorporation of additional silver substitution, yielding an idealized stochiometric formula of $AuAgTe_4$. A ternary diagram of the Au-Ag-Te system is shown in Figure 1.

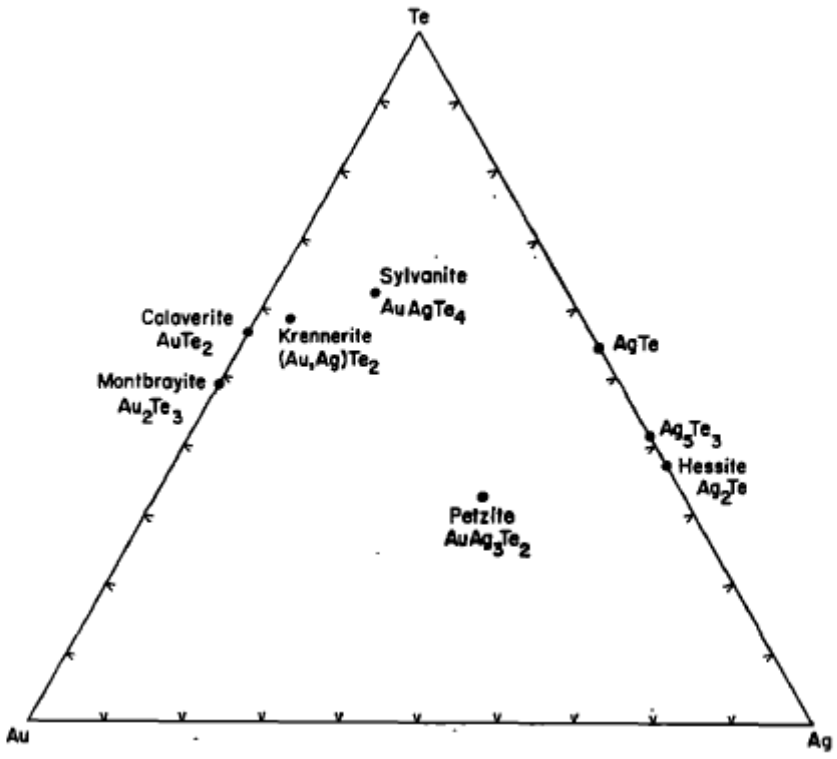

Figure 1: Ternary diagram of the Au-Ag-Te system

After Louis J. Cabri, 1965

Experimental Design:

In the last 25 years, many advancements have been made in the analytical techniques and refinement algorithms used in crystal structural studies. This prompted the author to undertake research aimed at redetermining and perhaps better resolving the atomic parameters of the primary gold telluride minerals. Research began by acquiring several gold telluride specimens from the University of Colorado's mineral collection. Several single crystals of calaverite were also kindly provided by Ed Raines, collections manager at the Colorado School of Mines Geology Museum. From these specimens and single crystals, sub-millimeter crystal mounts were prepared and tested in the laboratory of Dr. Joseph Smyth at the University of Colorado's Department of Geological Sciences.

Preparation of the crystal mounts consisted of removing small sections from the edges of larger crystals along fracture planes and other zones of preexisting weakness. This was done to minimize the effects of mechanical distortion that may have resulted from crystal removal through more aggressive means. These small crystal sections generally measured 25-100 µm on edge. Each crystal was cemented to the tip of a pulled glass filament using cyanoacrylate ("Super Glue"). The filaments were pre-mounted in small-diameter brass tubes using tack. Other crystal sections from the same parent crystals were retained in glass vials for later use in chemical determination studies.

The crystals mounted on glass filaments were mounted on an automated four-circle goniometer equipped with a Bruker APEX II CCD detector. The X-ray source was a Bruker rotating molybdenum (Mo K_α) anode X-ray generator operating at 50KV and 250mA. Each crystal underwent an initial diffraction scan which consisted of 72 ten-second exposure frames. These scans were conducted to determine the refinement potential of each crystal, with special attention placed on crystals which lacked any discernable mechanical deformation or uncharacteristic reflections produced from micro-twinning. Following each initial scan, the Bruker software algorithms were used to produce an initial estimate of the unit-cell of each sample based on the *hkl* data collected during the scan, verifying its identification as one of the gold telluride minerals. If the initial scans returned high quality data, intensity data were collected through a series of chi and omega scans covering a full sphere of reciprocal space to a two-theta maximum of 75°. These high resolution scans sought to refine the initial *hkl* dataset by comparing reflection positions and intensities across multiple scan sets, leading to a progressively lower R-value for the final integrated data. These long-duration scans were generally run overnight, as they take several hours to complete. The resulting integrated *hkl* file could then be used in later refinement.

Because initial data were collected using a CCD detector, the software algorithms are unable to produce a wholly precise measurement of axis-length and crystallographic angle. Therefore, a Bruker P4 point detector diffractometer was used to obtain the precise unit cell parameters of high-quality crystals, as ascertained from the initial scans. Following the acquisition of both the *hkl* file from the Apex II CCD detector, as well as the precise unit cell parameters from the point detector, the SHELXL (Sheldrick, 1997) refinement algorithm was employed to produce a full refinement of the atomic position parameters.

Grain Mounts and Polished Sections:

As a means of verifying the silver content of crystals used in the x-ray diffraction studies, small portions of the parent crystals were retained in glass vials for subsequent analysis as mentioned previously. These crystal fragments were prepared for analysis by creating grain mounts in the laboratory of Paul Boni at the Benson Earth Science Building. Grain mounts were prepared by suspending the crystal fragments in epoxy resin affixed to glass slides which were then allowed to cure for 24 hours in a heated oven at approximately 50° C. Upon curing, a diamond grinding wheel was used to smooth the surface of the epoxy, exposing the interior of the crystal grains. The surface of each grain mount was then refined through a grinding process which utilized 300 and 600 grit silicon carbide abrasive in a water slurry. Each mount was then hand polished using lapidary wheels impregnated with 6µm diamond grit. A final polish was applied using 0.05µm aluminum oxide.

In addition to the grain mounts, three polished sections and one polished thin section were prepared from specimen UMC No. 1641. This specimen was the source of the krennerite crystal which yielded a high precision structure refinement as discussed in later sections. To prepare the polished sections, three edges of the specimen were cut orthogonally to one another using a diamond tile saw. These sections were labeled 1641-1, 1641-2, and 1641-3 respectively. An additional cut was made parallel to the face which produced section 1641-1, and the material that was removed was made into a polished thin section for use in gangue/ore mineral association studies. Each polished section, as well as the polished thin section, were then planed and polished in a manner similar to that used in the grain mount preparation.

Electron Microprobe:

Each of the grain mounts, the polished sections, and the polished thin section were analyzed using wavelength dispersive spectroscopy (WDS) on a JOEL JXA-8600 Superprobe in the LEGS laboratory in the Benson Earth Sciences Building (Fig. 2). All scans were performed with standards for both Au and Ag. Te content was determined using the difference method. Secondary energy dispersive spectroscopy (EDS) was also utilized in each scan to ensure the Te values returned by WDS did not include other chalcophile elements such as Pb, Cu, Sb, etc. Backscatter electron images (BEI's) were also obtained during the analysis of the polished sections for use in later studies of paragenesis.

Figure 2: JOEL JXA-8600 Superprobe, LEGS Laboratory, Benson Earth Science Building

Optical Studies:

An optical study of the relationships between ore minerals in polished section included the analysis of several polished sections from the University of Colorado's Wahlstrom Collection that were analyzed for telluride mineral content, including section T-32 which will be discussed in detail in a later section. During the course of optical study, the polished mounts and polished thin section derived from specimen 1641 were analyzed in order to determine the paragenetic sequence of mineralization that led to the observed mineral assemblage. Each of the grain mounts prepared from material used in the XRD studies were also analyzed for homogeneity and the presence of indicative twinning.

In order to properly analyze the samples under the microscope, the author had to first learn the identification and analytical techniques relevant to reflected light microscopy. With the help of the University of Colorado's Department of Geological Sciences Mentorship Fund, the author attended a short course taught by Dr. John Lufkin at the Colorado School of Mines in the spring of 2010. During this course, the author learned the various optical attributes of the ore minerals as seen in reflected light, and also began to learn about the relationships of the various ore minerals based on specific occurrences. Information learned during this course was critical in later evaluation of the paragenetic sequence within specimens used in the XRD studies.

Krennerite Modeling:

Introduction:

In total, 14 single crystals from ten different specimens were analyzed using the APEX II CCD detector. Of these 14 crystals, three were used in long-duration χ and ω scans in order to produce high-resolution *hkl* data files. Of the three data files which were produced, only two yielded a satisfactory structural refinement accurate enough for publication, one each of calaverite and krennerite. Subsequent research focused primarily on the krennerite refinement, as it displayed a very high level of precision. Consequently, the modeling results presented in this section will focus only on the experimental data derived from this successful krennerite structural determination.

Krennerite, specimen 1641:

University of Colorado specimen UMC No. 1641 is shown in Figure 3. The specimen was collected from the Little Clara (Timber) Mine at Cripple Creek, Colorado by CU Regent H.D. Thompson sometime around the year 1900. The Little Clara Mine was owned by the Doctor-Jackpot Mining Company (mindat.org), and was part of the Doctor-Jackpot claim block, located northwest of the world-famous Cresson Mine. The specimen consists of bladed, subhedral, metallic crystals of sylvanite and krennerite up to 1.5 mm in length on a substrate of phonolitic volcanic tuff, sometimes referred to as a "breccia" in the historical literature (Lovering and Goddard, 1950). The sample itself was incorrectly labeled as calaverite, and was only found to contain krennerite after running an initial diffraction scan on a single crystal removed from the face of the specimen.

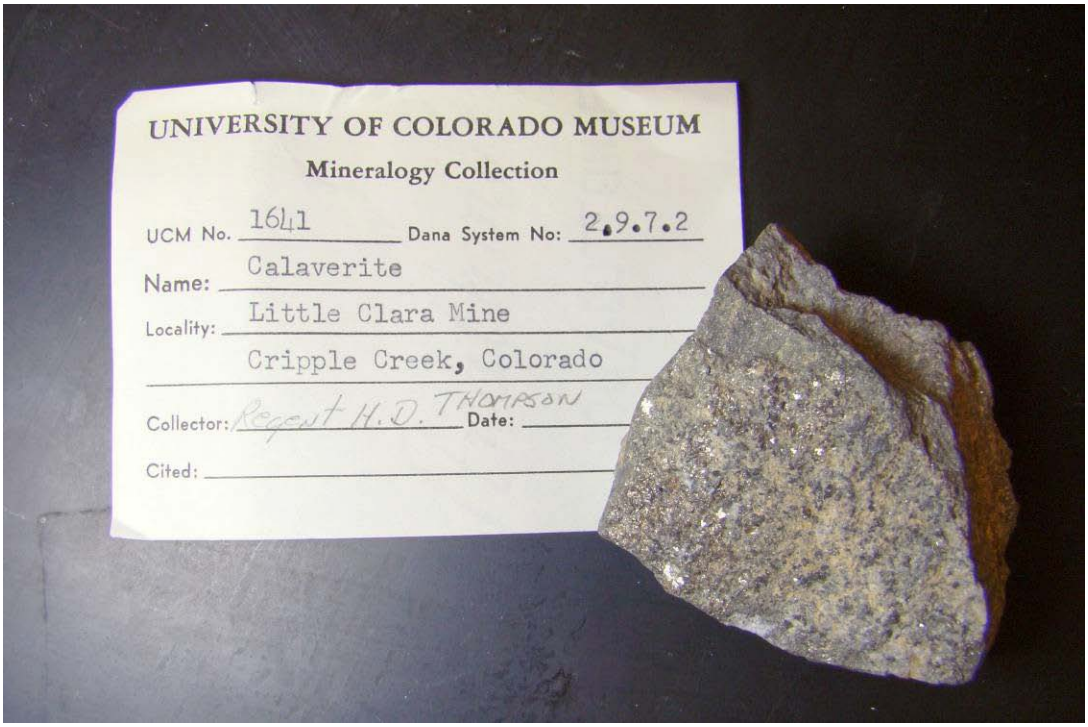

Figure 3: Specimen 1641, containing krennerite and not calaverite as labeled

Modeling Results:

An initial scan was run on a 25 x 25 x 6µm crystal removed from the face of specimen 1641. The unit cell data indicated that the crystal was in fact krennerite, and not calaverite as labeled. The Bruker software was then used to run a series of long-duration χ and ω scans in order to collect *hkl* data over a full sphere of reciprocal space. This full set of high precision *hkl* data was needed in order to produce a full structural refinement, as outlined previously. These long-duration scans produced a final *hkl* output file consisting of 18,882 reflections. Of these, 474 had intensities of less than 3σ, and were rejected from incorporation into the final refinement. Of the remaining 18,408 returned reflections, 3,406 were unique, and 3,150 of the unique reflections had intensities greater than 4σ. The unit cell parameters were refined using a Bruker P4 point detector diffractometer to give a = 16.590(3)Å; b = 8.867(2)Å; c = 4.4886(8)Å.

Atom position parameters were then refined using the SHELXL (Sheldrick, 1997) refinement algorithm. Atom parameters of Pertlik (1984b) were used for the initial structure. The structure refined to an R-factor of 0.11 using isotropic displacement parameters. Initial refinements gave a Flack X parameter of 1.0 whereas it should be near zero for the correct enantiomorph (Flack, 1983). The position parameters were then inverted and the Au1 z-parameter was set to zero to define the origin of the structure. Using anisotropic displacement parameters, the final refinement converged to an R-factor of 0.024 for the 3,150 unique reflections and 0.022 for the 1,901 unique reflections after merging. The resulting structure of krennerite is shown as an ellipsoidal model in Figure 4. Occupancies of the Au sites were modeled using neutral-atom scattering factors for gold, silver and tellurium. Occupancy refinements of these sites show that the structure is highly ordered with the Au1 position containing 43 atomic % Ag and 57% Au, the Au2 position containing 59% Ag and 41% Au, and the Au3 position consisting of pure gold.

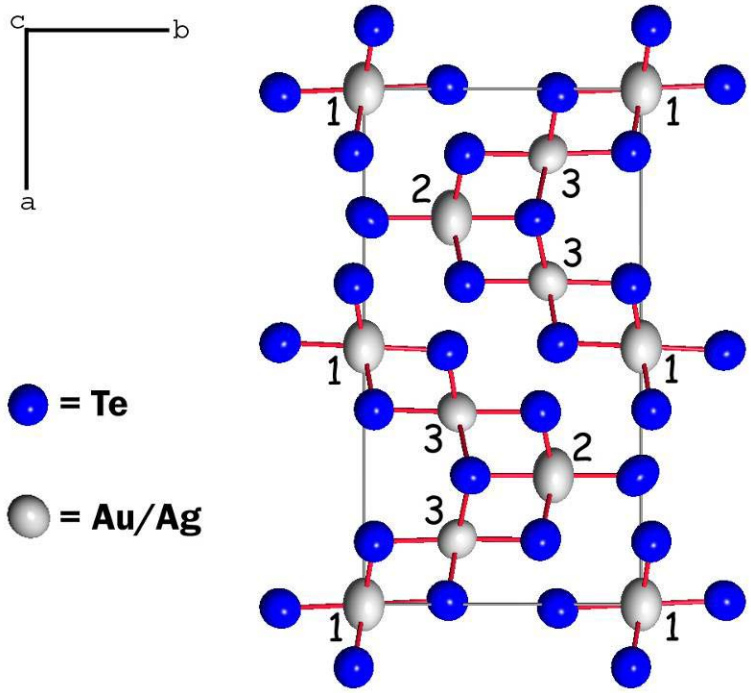

Figure 4: Ellipsoidal model of krennerite sample 1641 projected down [001]

Au-site numbers are labeled for reference

Final atomic position, anisotropic displacement, and occupancy parameters are given in Table 1. Table 2 lists the principle mean square atomic displacements for each atom.

Table 1: Fractional Coordinates, Occupancy, and Displacement Parameters for krennerite 1641

Atom	*x/a*	*y/b*	*z/c*	*Occ.**		*U11*	*U22*	*U33*	*U23*	*U13*	*U12*
Au1	0	0	0	0.574(4)	Au	0.206(2)	0.0122(2)	0.0227(2)	0	0	0.0015(1)
				0.426(4)	Ag						
Au2	0.75	0.68359(4)	0.99888(15)	0.413(4)	Au	0.0223(2)	0.0120(2)	0.0310(2)	-0.0002(2)	0	0
				0.587(4)	Ag						
Au3	0.87325(1)	0.33624(2)	0.51020(13)	0.999(2)	Au	0.0118(1)	0.0110(1)	0.0170(1)	-0.0010(1)	-0.0025(1)	0.0003(1)
Te1	0.75	0.98757(5)	0.05376(16)	1	Te	0.0127(2)	0.0132(2)	0.0165(2)	-0.0026(2)	0	0
Te2	0.75	0.38423(5)	0.13092(16)	1	Te	0.0106(2)	0.0119(2)	0.0153(2)	0.0005(2)	0	0
Te3	0.99237(2)	0.30122(3)	0.91175(17)	1	Te	0.0119(1)	0.0123(1)	0.0149(1)	0.0007(1)	-0.0007(1)	-0.0005(1)
Te4	0.87443(2)	0.63750(4)	0.53491(16)	1	Te	0.0130(1)	0.0117(1)	0.0174(2)	-0.0005(1)	0.0006(1)	-0.0005(1)
Te5	0.87800(2)	0.03659(4)	0.46689(15)	1	Te	0.0126(1)	0.0114(1)	0.0172(2)	-0.0002(1)	0.0010(1)	-0.0002(1)

**Occupancy factor*

Table 2. Selected inter-atomic distances and coordination parameters in krennerite.

Au1 Octahedron	57% Au; 43% Ag	Au2 Octahedron	41% Au; 59%Ag
Au1 – Te3(2)	2.6921(3) (Å)	Au2 – Te1	2.6956(6) (Å)
Au1 – Te5(2)	2.9207(5) (Å)	Au2 – Te2	2.7087(6) (Å)
Au1 – Te5(2)	3.1393(6) (Å)	Au2 – Te4(2)	2.9497(7) (Å)
		Au2 – Te4(2)	3.1847(7) (Å)
<Au1 – Te>	2.9174(5) (Å)	<Au2 – Te>	2.9484(5) (Å)
Polyhedral Vol	31.74 (Å^3)	Polyhedral Vol	32.67 (Å^3)
Oct. Ang. Var.	85.02	Oct. Ang. Var.	88.91
Quad. Elong.	1.032	Quad. Elong.	1.033
Au3 Octahedron	100% Au	Te – Te distances	
Au3 – Te2	2.6845(4) (Å)	Te1 – Te5 (2)	2.8419(5) (Å)
Au3 – Te2	3.4694(4) (Å)	Te3 – Te4	2.8248(6) (Å)
Au3 – Te3	2.6827(5) (Å)		
Au3 – Te3	3.3371(5) (Å)		
Au3 – Te4	2.6627(4) (Å)		
Au3 – Te5	2.6544(5) (Å)		
<Au3 – Te>	2.9151(5) (Å)		
Polyhedral Vol	31.63 (Å^3)		
Oct. Ang. Var.	52.24		
Quad. Elong.	1.044		

Discussion:

The structure of krennerite has the noble metal atoms in highly distorted octahedral coordination with Te. The octahedra form crenulated sheets that are connected only by common Te-Te bonds (Fig. 5). These same corrugated sheets are seen in the crystal structure of sylvanite, but they are more broadly arranged and positioned along a different crystallographic axis.

The structure reported here is essentially the same as that of Pertlik (1984b) except for the inversion of the absolute structure, which was needed to correct for the value of the Flack parameter. It is likely that both enantiomorphs are present in nature, but the crystal used in this study was small enough that only one was present in the sample. It remains unknown which depositional conditions favor one enantiomorph over the other. Despite the similarity of the reported structures, the current refinement yielded a six to ten-fold increase in the precision of the atomic position coordinates relative to the structure derived by Pertlik (1984b), thus providing the most detailed structural refinement of krennerite known to date. The improved precision was likely due to the large internal redundancy produced by collecting a full sphere of *hkl* data- a collection process that was not available to the previous researchers.

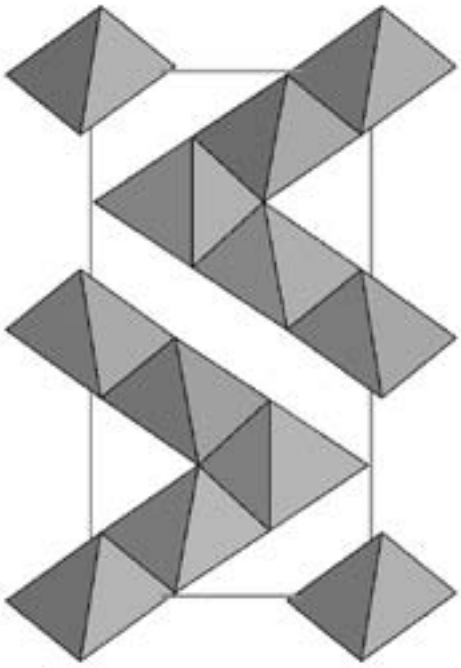

Figure 5: The polyhedral structure of krennerite projected down [001]. Note distortion of the octahedra.

Advances in analytical technique, including the efficiency of the refinement algorithms and the incorporation of the Flack parameter (Flack 1984), are factors that were also unavailable to either the Pertlik or the Tunell groups. All previous research utilized Weissenburg and precession film methods (Tunell & Murata 1950; Pertlik 1984), as well as powder diffraction photographs (Tunell & Murata, 1950). In addition to the precession film methods, Pertlik (1984b) utilized a point-detector diffractometer, the most advanced method of measurement available at that time. A comparison of the crystallographic constants derived in each study is summarized in Table 4.

Table 4: Comparison of crystallographic parameters from different studies of krennerite

	Tunell & *Murata* (1950)	*Pertlik* (1984)	This Research
a (Å)	16.54(3)	16.58(1)	16.590(3)
b (Å)	8.82(3)	8.849(5)	8.867(2)
c (Å)	4.46(3)	4.464(3)	4.4886(8)
volume (Å^3)	650.6	654.942	652.76
Density (g/cm^3)	8.86	n/a	8.749
Z	2	2	2
Space Group	*Pma*2	*Pma2*	*Pma*2
# of Unique Reflections	n/a	1063	3150
Minimum Intensity	n/a	2σ	3σ
R-value	n/a	5.80%	2.60%
Au wt. %	35.1	36.3	33.47
Ag wt. %	5.4	5.0	5.59

Paragenetic Data concerning Krennerite, Specimen 1641:

Paragenetic Data:

A brief paragenetic sequence was developed for specimen 1641 based on the textural relationships between krennerite and sylvanite as observed both visually using a reflected light polarizing microscope, and qualitatively using the electron microprobe's backscattered electron imaging function. Sylvanite was shown to be the most abundant telluride phase present in all of the polished sections, with krennerite representing the second most abundant telluride phase. The approximate ratio of optically observed sylvanite grains to optically observed krennerite grains was 5:1. A total of 20 krennerite grains were scanned in order to determine their silver content. In these scans, silver content ranged from 4.71-6.05 wt%, averaging 5.59 wt%. A total of 19 sylvanite grains were also scanned for the purpose of comparison, showing a silver range of 7.17-9.49 wt%. The average silver content of the sylvanite was 8.89 wt%. A polished thin section was also prepared to evaluate the relationships between the gangue and the ore minerals. The paragenetic sequence that was developed is shown in Figure 6.

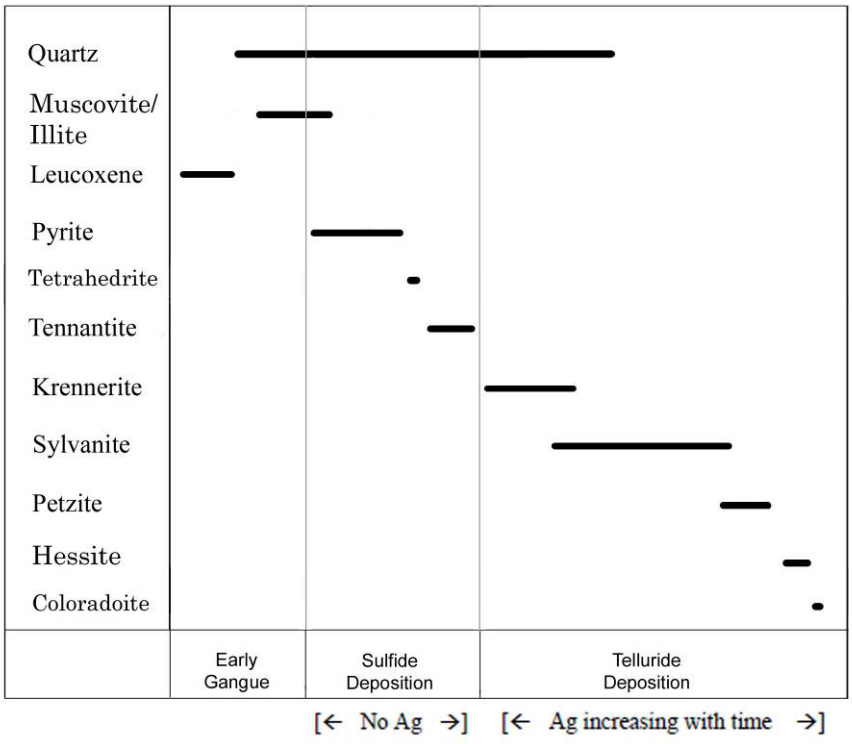

Figure 6: Inferred paragenetic sequence of sample 1641

Ore formation was characterized by early wall rock alteration and gangue mineralization, followed by sulfide deposition, and ending with late telluride formation. Both adularia-sericite alteration and pyritization were observed in the wall rock. Titanium was also apparently mobilized during alteration, allowing for the deposition of leucoxene group minerals during the early stages of gangue formation. Sulfide mineralization consists of early pyrite followed by slightly later tetrahedrite, which was then followed by Sb-rich tennantite. The tetrahedrite was only observed as 2-5µm corroded grains, suggesting partial resorbtion of the tetrahedrite during subsequent tennantite formation. The activity of Fe appears to drop as sulfide deposition progresses. This is evidenced by the crystal chemistry of the tetrahedrite and the Sb-rich tennantite, both of which lacked any discernable iron content when analyzed with the electron microprobe. Based on readings from the EDS, the tetrahedrite has the formula $Cu_{12}Sb_4S_{13}$ while the tennantite has the approximate formula $Cu_{12}(Sb,As)_4S_{13}$.

A lack of pyrrhotite formation during tetrahedrite/tennantite formation suggests that sulfur fugacity did not decrease with iron content (Dr. William Atkinson, Jr., personal communication). Instead, sulfur fugacity remained relatively constant, allowing for the preferential deposition of tetrahedrite/tennantite over the deposition of pyrite.

Sulfosalt precipitation was then followed by the deposition of gold and silver telluride minerals. Textural relationships suggest that available silver content increased with time, evidenced by the progressive increase of silver-rich telluride species present in the sequence. This relationship of increasing silver content with time is demonstrated in Figures 7 and 8, which show anhedral krennerite grains surrounded by optically continuous grains of sylvanite.

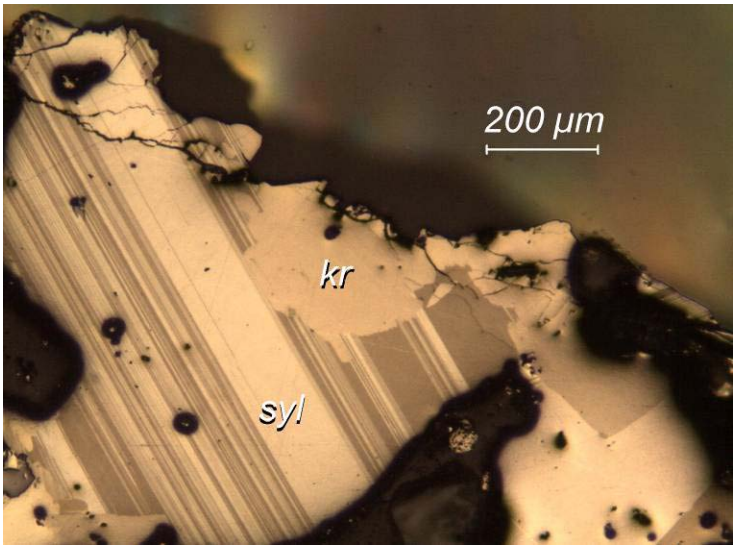

Figure 7: Specimen 1641-1: krennerite (kr) grain enclosed by optically continuous sylvanite (syl). Note the partial fragmentation of the krennerite grain prior to sylvanite mineralization. XP, 50x magnification.

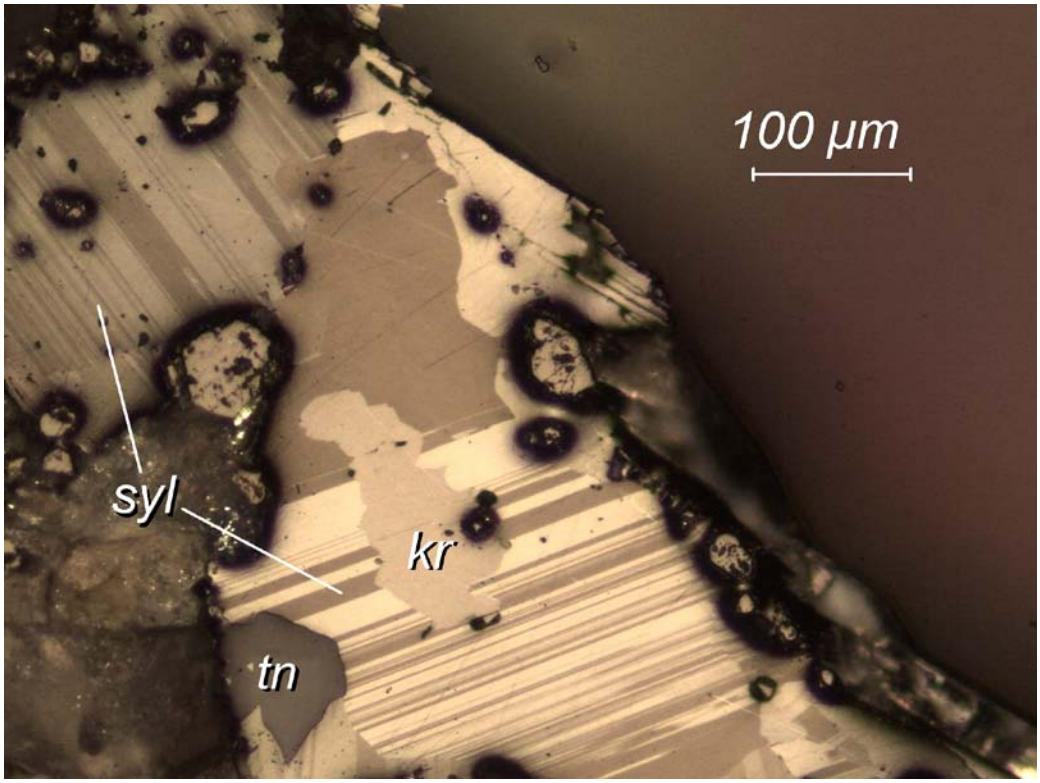

Figure 8: Specimen 1641-1: Krennerite grain enclosed by optically continuous sylvanite. Note the association with tennantite (tn). Crossed polars, 100x magnification.

This trend of early sulfide deposition followed by late telluride deposition fits well with the proposed paragenetic sequence of the Cripple Creek district as described by Lovering and Goddard (1950), and Saunders (1986). The relative path of telluride mineralization through time, as inferred paragenetically, is shown in Figure 9. In this figure, the path of telluride mineralization is superimposed upon a modified version of the phase diagram for the gold silver telluride minerals, as determined by Cabri (1965). In regard to telluride mineralization found in this sample, no fluid inclusion studies were performed. Therefore, no definite temperature constraints on telluride formation exist. Fluid inclusion data derived by Saunders (1986) on material from the Cresson Mine in Cripple Creek indicated a clustering of telluride-stage homogenization temperatures ranging from 150° to 175°C. However, this temperature range did not include any corrections for pressure due to uncertainties regarding the depth of formation, as well as the dominance of either hydrostatic or lithostatic pressure (Saunders, 1986, pg. 85). If a minimum pressure correction of 30°C is added to the temperature range described above, then the actual temperature range of telluride formation at the Cresson Mine would be 180° to 205°C.

The Little Clara Mine lies very close to the western edge of the Cresson Mine, so it is possible that the mineralizing fluids responsible for telluride deposition within specimen 1641 were of approximately the same temperature. The corrected temperature range of 180° to 205°C was therefore used to set the slope of the path of mineralization through time in Figure 9. The endpoints of the path shown were inferred using the microprobe results described previously.

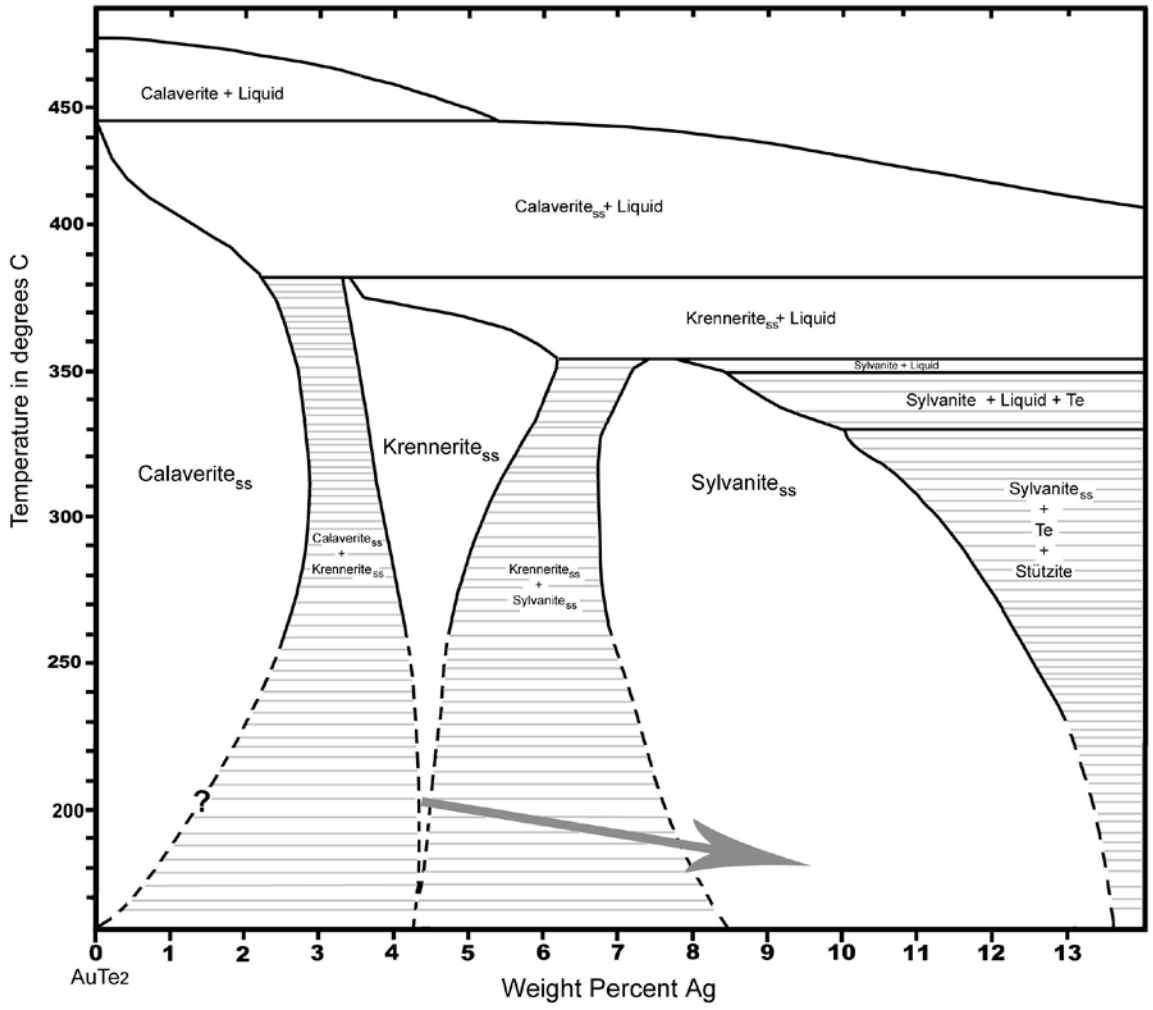

Figure 9: Path of telluride mineralization through time at Cripple Creek, CO.
Tie lines between coexisting mineral phases are shown in gray.
Modified After L.J. Cabri, 1965

It is important to note that the path of mineralization changes from krennerite-stable to sylvanite-stable with increasing silver content of the ore forming fluids. During the transition from krennerite to sylvanite deposition, the mineralizing fluids pass through a broad field in which both krennerite and sylvanite are thermodynamically stable. This intermediary stability field becomes wider with decreasing temperature, and is important in explaining the possible exsolution of sylvanite from krennerite, as discussed later in this section.

In the final stages of ore formation, sylvanite deposition appears to have caused the mineralizing fluids to become progressively depleted in gold, leading to the deposition of the silver-rich telluride species petzite ($AuAg_3Te_4$) and hessite (Ag_2Te). Paragenetically, the petzite appears to have preferentially formed at the perimeter of large sylvanite crystals, in the last remaining free space of the vugs in which the sylvanite had formed. Petzite was also observed in contact with smaller crystals of both sylvanite and tennantite. Where in contact with sylvanite, the two species share a common grain boundary. This suggests that petzite began to form as the result of a continued drop in available gold content with time, which would have rendered further sylvanite crystallization unstable. Note that petzite is not included in the phase diagram shown in Figure 9, although it has been proposed that sylvanite and petzite may form contemporaneously under specific conditions of low temperature (Cabri, 1965). Photomicrographs demonstrating the common relationship between sylvanite, petzite and tennantite are shown in Figures 10 and 11.

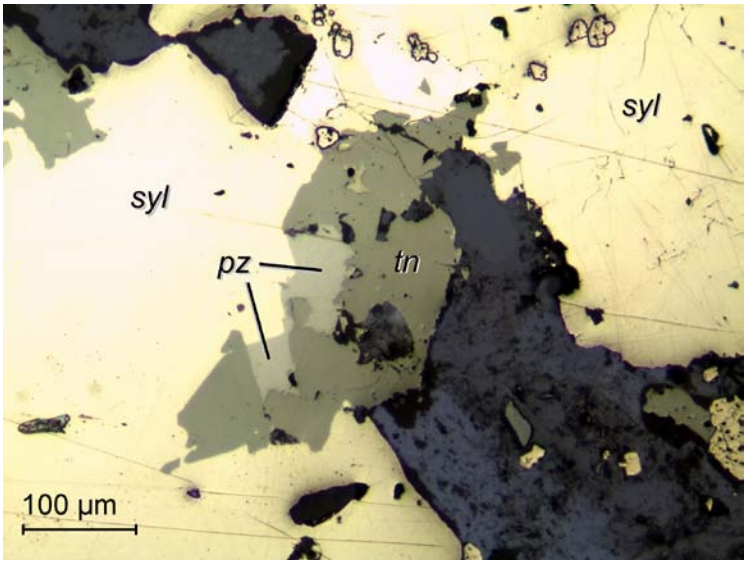

Figure 10: Photomicrograph of sylvanite (syl), petzite (pz) and tennantite (tn) in specimen 1641-T. Plane Polarized Light, 100x magnification.

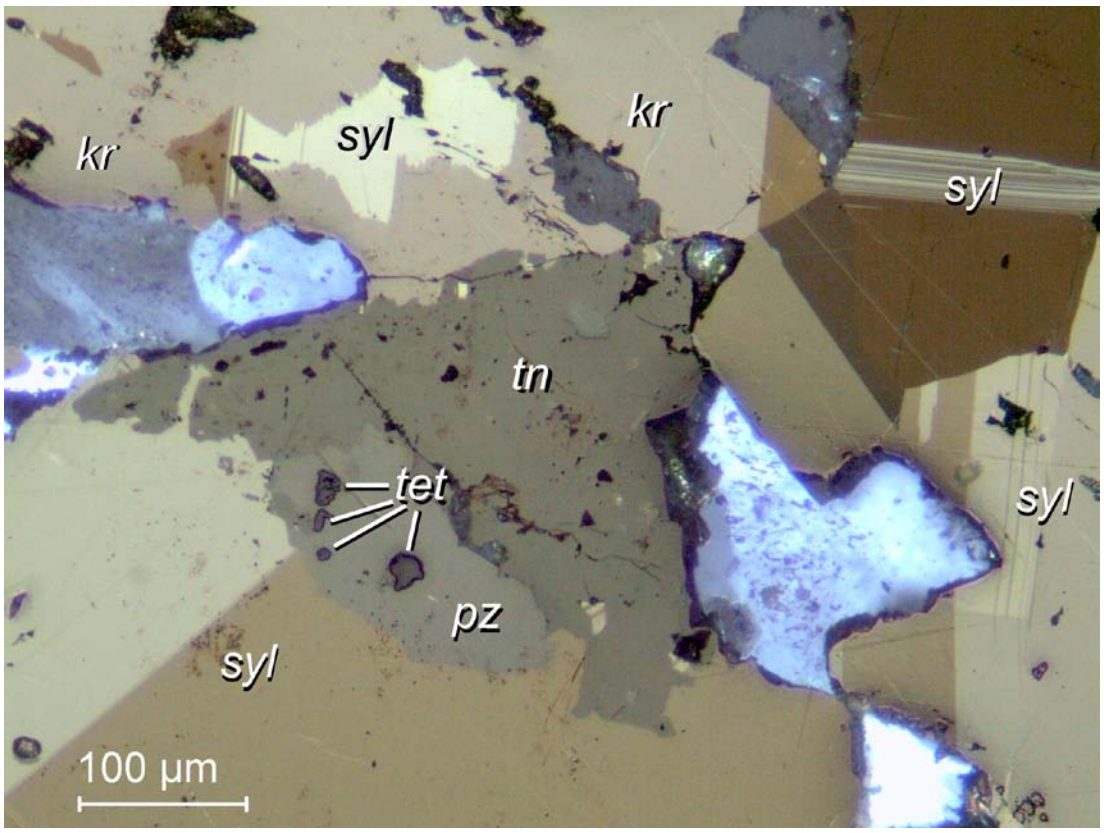

Figure 11: Photomicrograph of sylvanite (syl), petzite (pz), tennantite (tn), and tetrahedrite (tet) in specimen 1641-T. Sylvanite can be seen backfilling a cavity in krennerite (kr).
Crossed polars, 100x magnification.

Notes on Possible Exsolution:

During the development of the paragenetic sequence, a single grain of krennerite was observed to contain what appeared to be exsolution lamellae. The lamellae are aligned parallel to one another within an otherwise homogeneous grain of krennerite, as shown in Figure 12. These lamellae were not immediately obvious in plane polarized light, yet became very distinct under crossed polars. In order to analyze the chemical composition of these lamellae, several points were analyzed with the electron microprobe. The krennerite grain was also analyzed in two locations to verify its visual identification. The lamellae returned silver contents of 7.17 to 7.71 wt%, well within the range of silver content of sylvanite. The enclosing grain returned a value of 5.81 wt% Ag, consistent with krennerite. Secondary EDS was again utilized to ensure that non-stochiometric elements were not included in the returned values. To the best of the author's knowledge, sylvanite exsolution from krennerite has not been previously reported. However, the morphology of the lamellae seen here is indeed suggestive of exsolution. It is possible that the sylvanite replaced portions of a previously existing krennerite grain through the diffusion of silver, but if so, one would expect irregular grain shapes rather than the lamellar texture. Furthermore, the intermediate stability field between krennerite and sylvanite, as discussed previously, would permit for the exsolution of sylvanite from krennerite, and vice versa (Louis J. Cabri, personal communication).

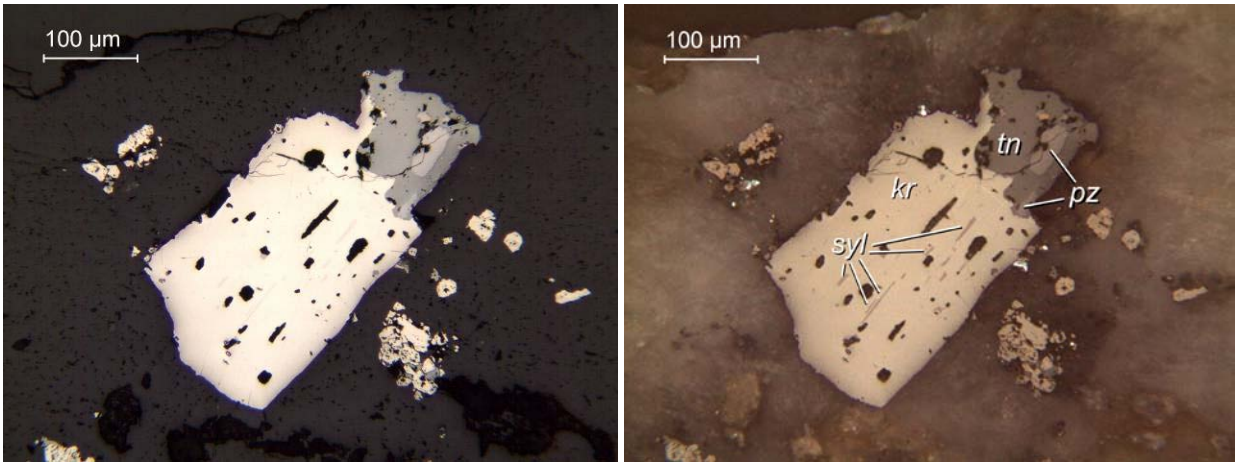

Figure 12: Possible exsolution lamellae of sylvanite in krennerite. The left photomicrograph is in plane polarized light, while the right is in crossed polars; Specimen 1641-2, 100x magnification.

A final piece of evidence for the plausibility of exsolution comes from the structures of krennerite and sylvanite themselves. The two structures are similar in the coordination and arrangement of the Au and Ag atoms, despite their differences in crystal system and space group.

The presence of exsolution lamellae would imply that the two species coexisted and that the composition ranges of each became more restrictive on cooling (Fig. 9). Therefore, I hypothesize that the intermediate stability field not only allows for the simultaneous deposition of krennerite and sylvanite, but that within this field, it is possible to form metastable krennerite or sylvanite crystals, which contain an excess of silver or gold, respectively. Upon cooling, these metastable grains would exsolve the corresponding species in order to attain thermodynamic stability. The dominant mineral within a given exsolution assemblage will then be dependent upon the direction by which the ore forming fluids enter the field. Those entering the intermediate field from the silver-poor side on the left will show dominantly krennerite with minor sylvanite exsolution, as seen here. Fluids entering from the silver-rich side to the right, however, should have sylvanite as the dominant mineral, with minor krennerite exsolution.

It is unlikely that the exsolved mineral will ever represent anything more than a minor phase, which may be why there are few, if any, previously validated reports of krennerite-sylvanite exsolution in the literature. It is unknown if exsolution is possible within the calaverite-krennerite intermediate field, but it seems less likely due to the more significant structural differences between the calaverite and krennerite species.

It should be noted that morphology and theory alone do not prove exsolution. It is also possible that the sylvanite lamellae represent epitaxial growth upon a grain of krennerite, or that the telluride minerals are replacing some previously existing mineral phase that had distinct parallel cleavage upon which the sylvanite was able to nucleate. Further testing with transmission electron microscopy would be needed in order to reach any definite conclusions, although the evidence here is most suggestive of exsolution.

Special Studies:

During the course of this research, several other structural studies were performed on the two remaining gold (silver) telluride species, calaverite and sylvanite. Redetermination of the unit cell of calaverite was quite successful, though a large degree of positional uncertainty was seen in the tellurium atoms upon refinement. Redetermination of the sylvanite cell met with less success. Of special interest in this section is the reanalysis of the crystal chemistry of the indeterminate calaverite/krennerite phase first described by Geller (1993). Data concerning this new analysis can be found in the last portion of this section.

Calaverite Modeling, introduction:

In addition to the krennerite modeling discussed earlier, several crystals of calaverite were also analyzed in attempt to redetermine the unit cell and refine the structural parameters of the species. Two primary crystals were used in this portion of the study. The first came from specimen 1888 in the university's mineral collection, and the second was loaned for study by Ed Raines, collections' manager at the Colorado School of Mines Geology Museum.

Specimen 1888 was collected in the Gold Hill Mining District of Boulder County, Colorado. The name of the mine which produced the specimen is unknown. The specimen consisted of thin, prismatic crystals of calaverite in a feldspar-rich, phaneritic granitoid matrix (Figures 13 and 14). Telluride mineralization was strongly associated with pseudomorphic "mustard gold" within parallel mineralized seams. Mustard gold is a product of the oxidation of calaverite, leaving behind a porous mass of immobile gold whose color resembles that of mustard, suggesting that the specimen came from the oxidized zone of an ore body. As a note, the specimen is labeled as occurring with rusty gold, but this is a term usually associated with the oxidation product of sylvanite, and not calaverite. Seams of potassium feldspar and quartz run parallel to the mineralized veins.

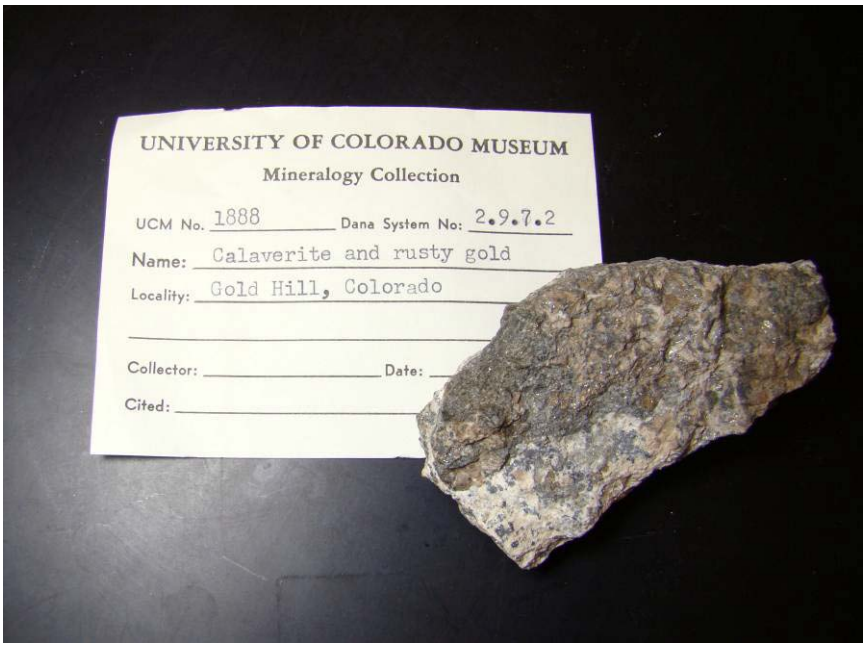

***Figure 13*:** Specimen 1888, Gold Hill Mining District, Boulder County, Colorado

***Figure 14*:** Close-up of mineralized veins in specimen 1888

The specimen on loan from Ed Raines came from the Cripple Creek Mining District of Colorado, and consisted of a single, euhedral crystal of calaverite measuring approximately 5mm in length. This crystal was labeled ER-2 for reference. The crystal showed a perfect 7-point angular termination, and was specifically chosen for study based on its euhedral form.

Calaverite Modeling, Results:

Small cleavage fragments were removed from each parent crystal, and each was subjected to an initial scan using the APEX II CCD detector. Although visually identified as calaverite, the crystal harvested from specimen 1888 did not return a proper unit cell. Several attempts were made by Dr. Smyth and myself to transform the orientation matrix so that proper unit cell parameters could be derived. This led to a final point detector unit cell approximation of a = 7.648(10)Å; b = 4.289(8)Å; c = 10.119(9)Å; β=90.43°. This unit cell approximates the accepted unit cell of calaverite, a = 7.1947(4)Å; b = 4.4146(3)Å; c = 5.0703(3)Å; β=90.03° (Schutte and De Boer, 1988), but its length is doubled along the c-axis. The derived unit cell parameters, combined with indexing in the *hkl* file, indicated that the crystal was most likely calaverite ordered with extra reflections, leading to this doubled length. These extra reflections resulted from some kind of internal defect that prevented the acquisition of the proper unit cell. This defect may have been due to mechanical deformation or, more likely, from microtwinning within the crystal. The latter may have caused several of the reflections to deviate from their expected locations, ultimately leading to an inaccurate unit cell determination. At least two other crystals from specimen 1888 were also scanned, but neither produced a viable unit cell for calaverite.

Since the calaverite in specimen 1888 was strongly associated with mustard gold, it may also be possible that the improper unit cell was the result of an incoherent crystal structure brought about through partial oxidation. The crystals used in the study were specifically chosen to not contain any visible degradation on either the crystal or the immediately surrounding regions. However, this does not preclude crystal degradation on the atomic scale.

Unable to produce a viable unit cell refinement from specimen 1888, attention was turned to crystal ER-2. As with previous material, a small cleavage fragment was removed from the larger crystal for study. Cell parameters from an initial scan indicated the crystal was in fact sylvanite. However, it was noted that the returned beta angle was 125.1°, whereas it should have been near 90.03° for calaverite.

A transformation was applied to correct the beta angle, and a full *hkl* dataset was collected during an overnight scan set. The unit cell was then refined on the Bruker P4 point detector. The final unit cell for ER-2 was a = 7.2252(6)Å; b = 4.4381(3)Å; c = 5.0788(4)Å; β = 90.83°. This determination was in close agreement with the accepted parameters for calaverite, and therefore represents an accurate redetermination of the calaverite unit cell.

Following acquisition of this data, and with the help of Mr. Yu Ye, the author ran a refinement of the crystal structure using SHELXL (Sheldrick, 1997) in order to observe the atomic position coordinates for comparison with previously published structures. It was quickly noted that the tellurium atoms had a positional uncertainty of nearly one order of magnitude greater than the uncertainty for the gold and silver atoms. A model of the atomic structure of crystal ER-2 was created using XtalDraw for the means of visualization, and is shown in Figure 15. Note the gross elongation of the tellurium atoms, which appear as blue "cigars". The shape of the tellurium atoms in the ellipsoidal model is the direct result of the large positional uncertainty of the tellurium atoms within the refined structure. It is believed that this uncertainty is the result of the incommensurate modulation of silver within the calaverite cell.

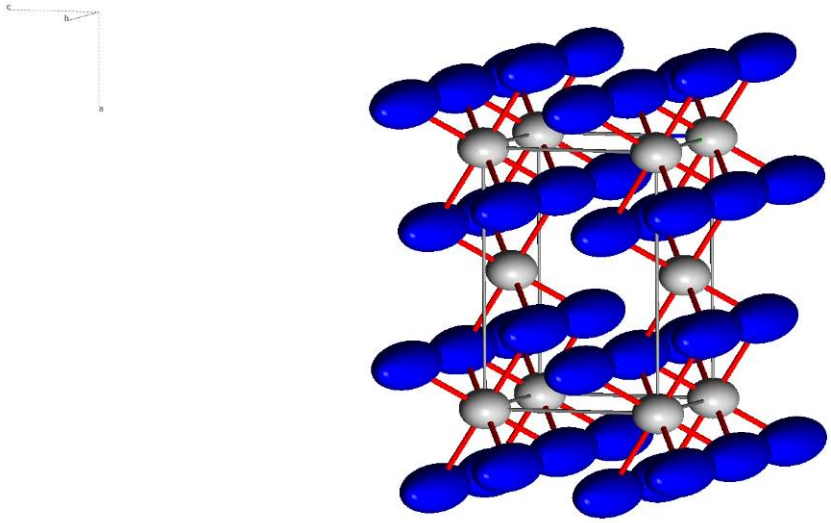

Figure 15: Ellipsoidal model of calaverite ER-2

In essence, silver appears to be randomly substituted for gold within the calaverite cell up to a threshold of approximately 3 wt% (Schutte and De Boer, 1988; Bindi et. al, 2009). This is what is meant by the term 'incommensurate modulation'. It appears that this randomized silver substitution does not have an effect on the position of the gold and silver atoms within the crystal structure, but instead has a direct effect on the bond angle between the gold and silver atoms and the adjoining tellurium atoms. This effectively causes the tellurium atoms to shift in position along one axis. Because refinement algorithms attempt to average the position of the atoms, the result is a cigar shape that represents all of the possible positions of the tellurium atom across multiple unit cells. Using the available modeling techniques, we were unable to rectify the positional uncertainty displayed by the tellurium atoms. It is interesting to note that the calaverite structure derived by Schutte and de Boer (1988) also contains a large positional uncertainty in the tellurium atoms, as shown in an ellipsoidal model of their unit cell in Figure 16.

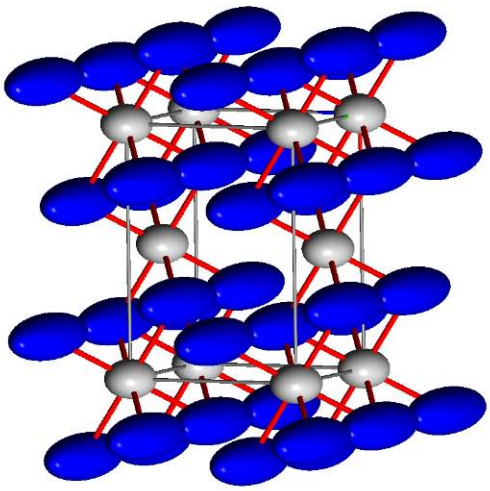

Figure 16: Ellipsoidal model of calaverite, after Shutte and De Boer (1988)

Newer research by Bindi et. al (2009) yielded a means of accurately determining the position of the tellurium atoms across multiple iterations of the unit cell through the utilization of a superspace modeling technique that was not available to us. Through their work using this superspace technique, the Bindi group (2009) were able to show definitively that silver is not coherently substituted for gold within the unit cell, which would have resulted in rhythmic substitution across multiple cell iterations. Instead, silver appears to be randomly substituted up to the threshold of approximately 3 wt%. An ellipsoidal model of calaverite based on data derived by Bindi et. al is shown in Figure 17. This model is based on structural parameters for calaverite "$Ag_{0.09}$", whose refinement yielded a low reliability factor (R-value) of 0.0426.

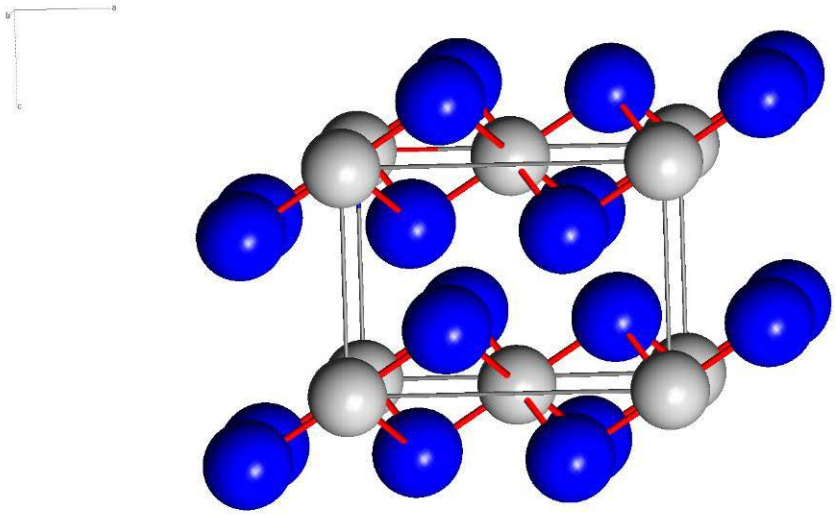

Figure 17: Ellipsoidal model of calaverite

After Bindi et. al (2009)

Sylvanite Modeling:

The last species to be examined using x-ray diffraction techniques was sylvanite. Early in the course of the research, it was realized that sylvanite could be potentially problematic due to its characteristic polysynthetic twinning. Within the sylvanite structure these twins tend to be very closely spaced, greatly increasing the chance of obtaining poor quality diffraction data due to the extra reflections that would result from an intergrown twin structure. In attempt to minimize this effect, several polished sections from the Ernest Wahlstrom collection at the University of Colorado were visually analyzed for the presence of sylvanite grains that contained wide twin spacing. More than 20 sections were analyzed, and only one contained blades of sylvanite that had twin spacing of greater than 300μm. This was section T-40 from the Boulder County Mining District of Colorado, shown in Figure 18. The exact mining district which produced this specimen is unknown. A photomicrograph of the wide twin spacing is shown in Figure 19.

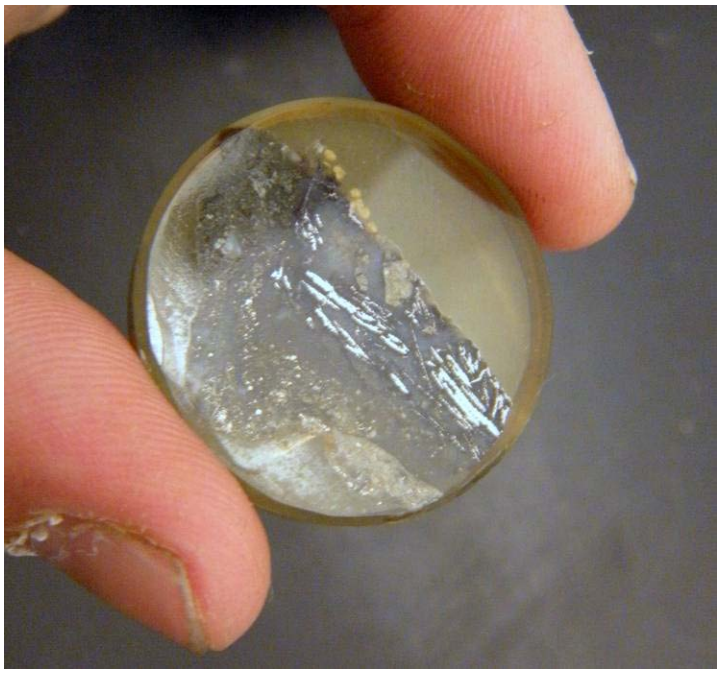

Figure 18: Polished section T-40 from the Wahlstrom Collection. Note the large sylvanite blades.

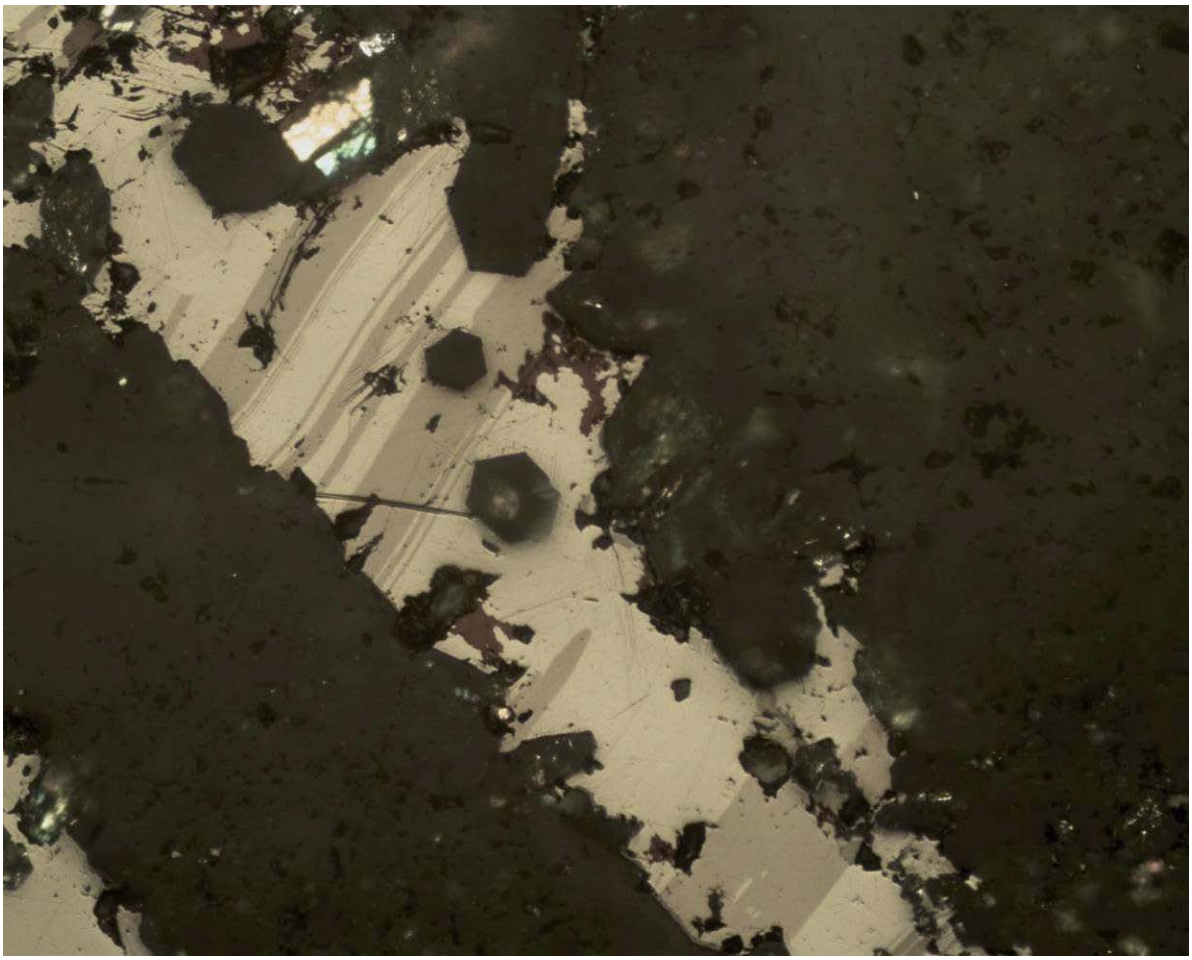

Figure 19: Polysynthetic twinning in sylvanite, seen within a quartz matrix. Section T-40. Field of view is approximately 1mm. Crossed polars, 100x magnification. Note wide twin spacing.

Ideally, the sylvanite crystal used in the XRD study would be free of twin planes. As section T-40 contained such wide spacing between twin planes, permission was received to remove a portion of one of the sylvanite crystals using a microscope-mounted drill. The drill setup is shown in Figure 20. This drill was used to remove a 2x2 mm block from the face of the section, which was then broken down further to produce an untwined crystal of sylvanite for analysis.

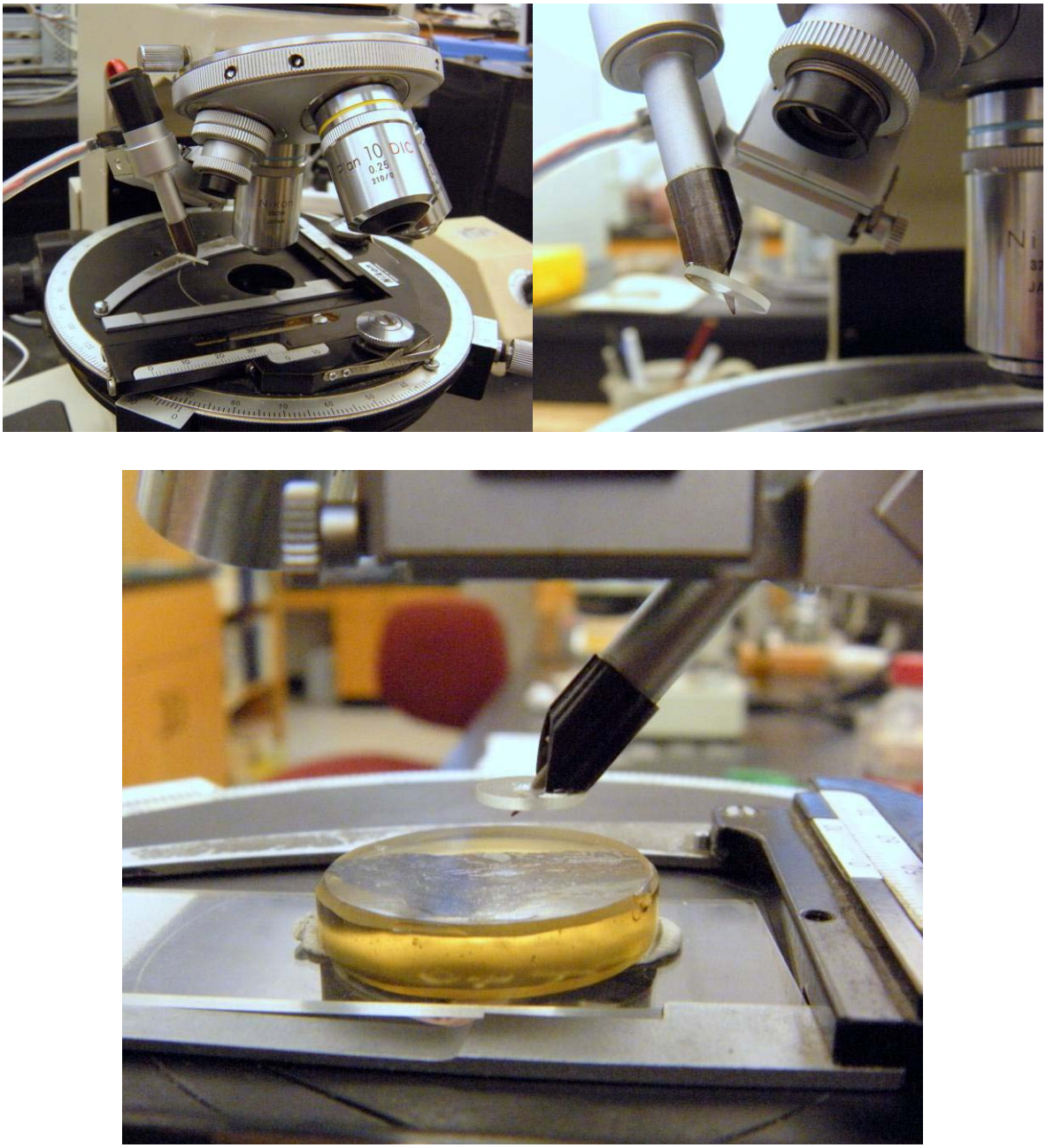

Figure 20: Scope-mounted drill assembly used to remove a portion of sylvanite from T-40.

Four untwinned sylvanite crystals were harvested from the small block that was removed from the face of the polished section. All four of these crystals underwent an initial scan using the APEX II CCD detector. Despite the extreme care taken while extracting the crystals, each of the scans returned a series of curvilinear reflection profiles, as opposed to the single spot reflections that would be needed in order to determine the structural parameters of the sylvanite unit cell. These curved reflections could have only resulted from internal mechanical deformation of the crystal during the extraction process. Because all four of the crystals prepared from the extraction showed this mode of deformation, and because other crystals harvested from specimens of graphic sylvanite returned unusable data due to pronounced polysynthetic twinning, it was decided to abandon the sylvanite refinement.

Indeterminate Calaverite/Krennerite Composition:

During his doctoral research, Dr. Bruce A. Geller first described an indeterminate gold telluride phase in an ore mount from the Alpine Horn Mine in the Sugarloaf Mining District of Boulder County, Colorado. This indeterminate phase was also observed in polished mounts prepared from material in the Mud Vein at the Logan Mine, The Golden Harp Mine, the Poorman's Relief Mine, the Orofino Mine, the Lady Franklin Mine, and the Nancy Mine, all of which are located in the Boulder County telluride belt. Without XRD data, the easiest way to distinguish between the three primary gold and silver telluride minerals is through electron microprobe analysis. Ascertaining silver content allows one to distinguish between the three primary species. However, this approach does not always achieve an expected result.

The phase discovered by Dr. Geller was specifically labeled as 'indeterminate' because it contains silver atomic weight percentages that lie between the upper threshold for historically observed (and theoretically calculated) silver content in calaverite, yet below the accepted minimum value of silver content in krennerite. Hence, the phase was labeled as "indeterminate calaverite/krennerite", or "ind ca/kr" (Geller, 1993).

In addition to characteristically containing a non-diagnostic silver content when analyzed using wavelength dispersive spectroscopy, the indeterminate phase also has several unique optical properties. Both the minimum and maximum reflectivities of the indeterminate phase deviate from those of either calaverite or krennerite. More importantly, the reflectivity profile of the indeterminate phase, as measured in 20nm increments from 480nm t0 620nm, has a gross change in shape when compared to

the profiles of either krennerite or calaverite. The shape of the reflectivity profile is of more significance than the actual reflectivity values (Bruce Geller, personal communication). Consequently, the variable shape of the indeterminate calaverite/krennerite profile, as compared to either the calaverite or krennerite profiles, is sufficient evidence to suggest that this phase is indeed indeterminate (Geller, 1993).

Two samples containing grains of the indeterminate phase were scrutinized by Dr. Geller for their silver content using wavelength dispersive spectroscopy. These were samples PMR 83-10 from the Poorman's Relief Mine and T-32 from the Alpine Horn Mine, as published in his dissertation. These two samples showed a silver content range of 3.02 – 3.68 weight % and 2.68 – 4.28 weight %, respectively. The average silver content of the indeterminate phase in PMR 83-10 was 3.45 weight %, and the average in T-32 was 3.61 weight %. Both of these values lie above the upper theoretical threshold of silver content in calaverite as calculated by Cabri (1965), yet lie below the minimum threshold of 4.7 weight % silver that has been historically observed in krennerite specimens within published accounts (Cabri, 1965;Pertlik, 1984b). Therefore, it can be summarized that the silver content of the indeterminate phase lies within the miscibility gap between calaverite and krennerite.

During the course of the current research, I came across section T-32 while sorting through polished sections used in Dr. Geller's research. Dr. Geller and I were able to relocate the exact location within the mount where he had taken his data points nearly 20 years prior. A photomicrograph of the indeterminate phase is shown in Figure 21. Note that the sinuous lamellae of the indeterminate phase has formed at right angles to larger sylvanite twin lamellae, a fact first noted by Dr. Geller during his doctoral research. The lamellae of the indeterminate phase have the appearance of those produced through exsolution, and have a texture that may suggest replacement.

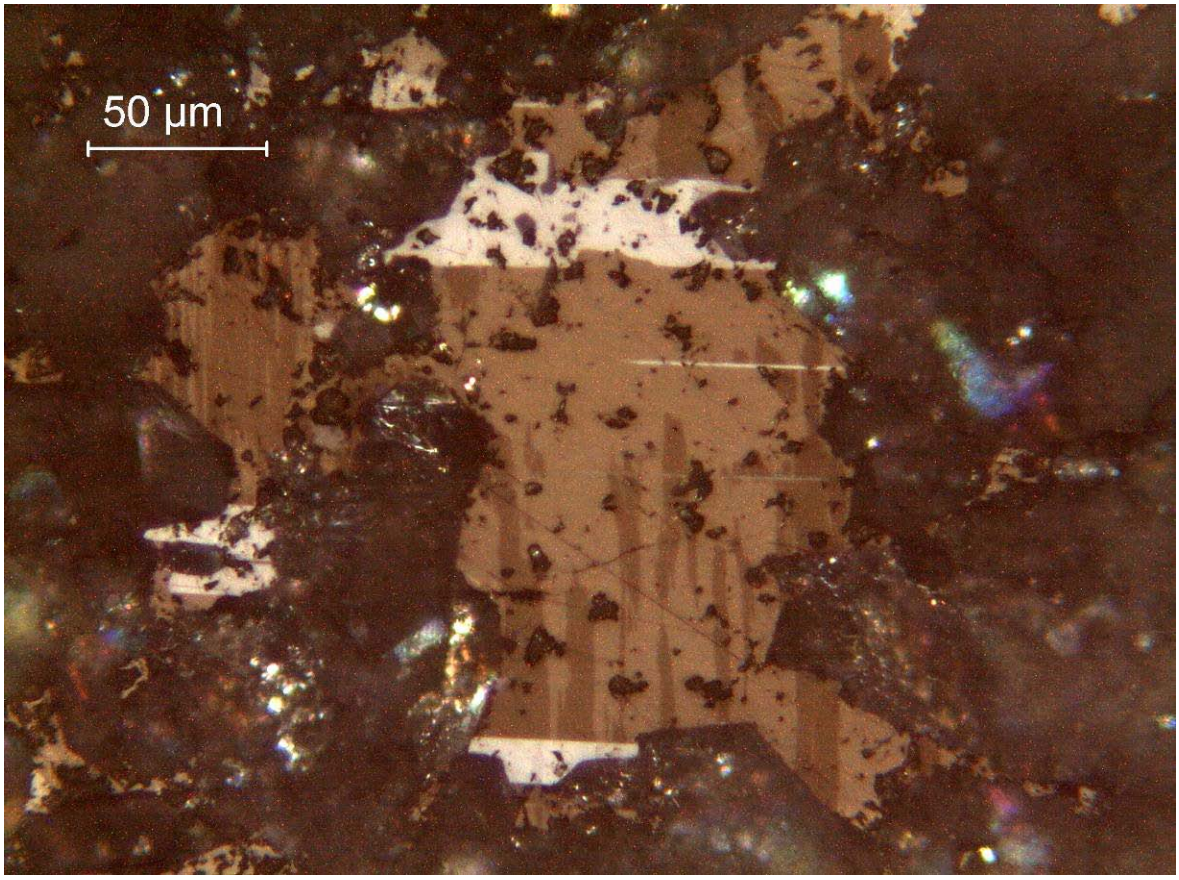

Figure 21: Grain of Indeterminate calaverite/krennerite in polished section T-32. The indeterminate phase is darker in color than the enclosing sylvanite, and has formed at right angles to larger sylvanite twin lamellae, seen here as the white strips. Crossed polars, 200x magnification.

Having found the grain which had been previously tested, the sample was reanalyzed using the electron microprobe in order to define the grain chemistry at several additional points. Systematically, each of the darker lamellae of the indeterminate phase were analyzed, as were the lighter portions of the grain which lie between the darker lamellae. In all, 13 points were analyzed using the electron microprobe. Figure 22 contains a summary of the results from these analyses. As demonstrated, the indeterminate phase contained a remarkably homogeneous silver content, as did the enclosing grain of sylvanite. Similar to the results of Dr. Geller, the indeterminate phase was shown to have an average silver content of 3.33 weight %- Dr. Geller's analysis showed an average of 3.61 wt% Ag. The enclosing sylvanite had an average silver content of 8.73 weight %.

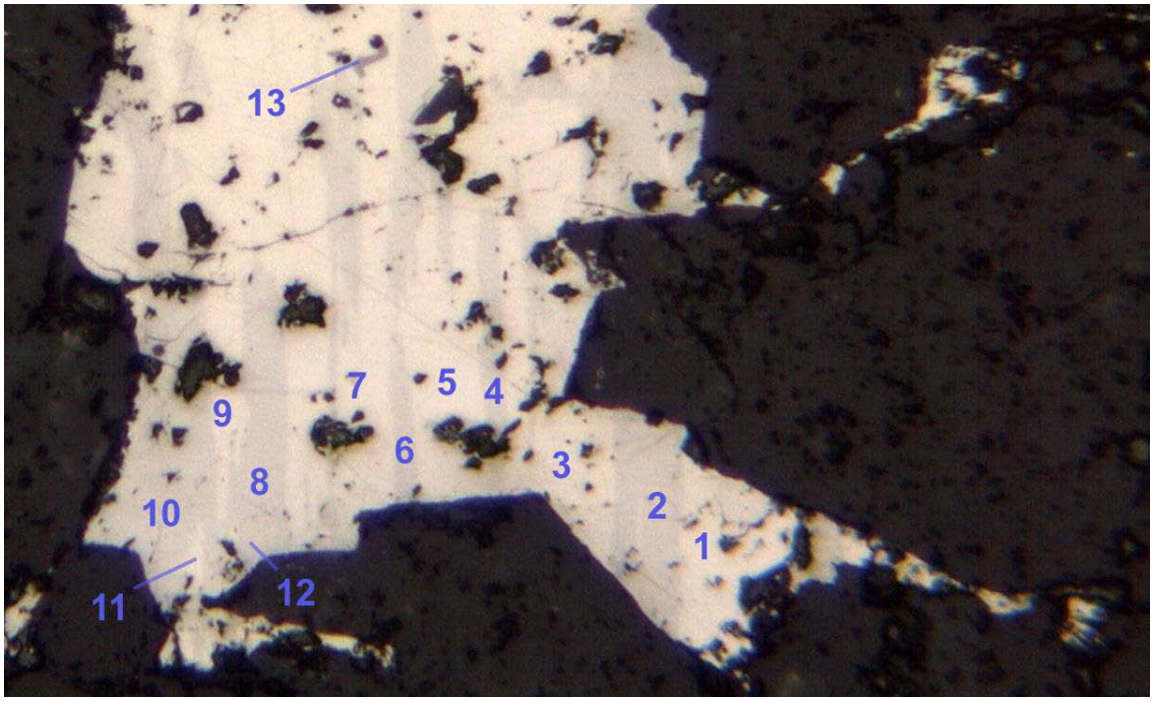

Pt #	Te	Au	Ag	Total	ID
1	59.8	36.83	3.37	100	ind. Ca/Kr
2	62.35	28.35	9.3	100	sylvanite
3	60.08	36.76	3.16	100	ind. Ca/Kr
4	62.25	28.78	8.97	100	sylvanite
5	60.08	36.73	3.19	100	ind. Ca/Kr
6	61.73	29.69	8.58	100	sylvanite
7	58.67	37.15	3.77	100	ind. Ca/kr
8	61.88	29.65	8.47	100	sylvanite
9	59.46	37.48	3.06	100	ind. Ca/Kr
10	61.01	30.64	8.35	100	sylvanite
11	59.4	37.18	3.42	100	ind. Ca/Kr
12	62.96	28.35	8.69	100	Sylvanite
13	0	0	0	0	Tennantite (CuAsS on EDS)

Figure 22: Photomicrograph of points analyzed in polished section T-32 with accompanying probe data. All values are in atomic weight percent. Plane polarized light, 400x magnification.

It remains unknown which species the indeterminate phase actually represents. The silver content cannot be used to discern this fact. Furthermore, the difference in the reflectivity profile of the indeterminate phase suggests that it is neither wholly calaverite, nor krennerite. Based on these differences within the reflectivity profile, it may be possible that the indeterminate phase represents a previously undescribed metastable phase, or perhaps even a new mineral species, although it may also represent a sub-microscopic intergrowth of krennerite and calaverite. The texture of the indeterminate phase seems to suggest that it has replaced sylvanite, although it is also possible that the lamellae were derived from exsolution.

In truth, there are many possible explanations for the ambiguous nature of the indeterminate phase, and the data presented here does not support any one of these hypotheses over another. The only sufficient means to ascertain the true nature of the indeterminate phase would seem to lie in the study of its crystal structure. Because the phase has formed as micrometer-scale lamellae, and given the mechanical distortion caused by attempting to remove sylvanite grains from a polished section as discussed previously, removal of the indeterminate phase for single crystal examination is implausible. It may be possible to mill a portion of the indeterminate phase for further testing on a transmission electron microscope, which would allow for observation of symmetry operators and thus allude to its crystal structure, but this technique was outside of the purview of this study. Consequently, the indeterminate phase will have to remain indeterminate, at least for now.

Acknowledgements:

I would like to thank Paul Boni, Dr. John Lufkin, Dr. John Drexler, and Mr. Yu Ye for providing me with the training necessary to complete this study. I would also like to thank Ed Raines for sharing both his time and enthusiasm for the telluride minerals, as well as for the many stimulating conversations derived therein. Thanks are also extended to Dr. Lang Farmer for his help with arrangements to take Dr. Lufkin's course in reflected light microscopy. Finally, very special thanks are extended to my advisors, Dr. Joseph R. Smyth, Dr. William W. Atkinson Jr., and Dr. Bruce A. Geller. It was your generosity of wisdom and words of encouragement that made this study a truly wonderful experience.

References

Bindi, L., Arakcheeva, A., Chapuis, G. (2009) The role of silver on the stabilization of the incommensurately modulated structure in calaverite, $AuTe_2$. American Mineralogist, Vol. 94, 728-736

Cabri, L.J. (1965) Phase relations in the Au-Ag-Te system and their mineralogical significance. Journal of Economic Geology, 60, 1569-1606

Flack, H.D. (1983) On enantiomorph-polarity estimation. Acta Crystallographica, A39, 876-881

Geller, B.A. (1993) Mineralogy and origin of telluride deposits in Boulder County, Colorado, 731 p. Ph.D. thesis, University of Colorado, Boulder.

Lovering, T.S. and Goddard, E.N. (1950) Geology and Ore Deposits of the Front Range, Colorado. Geological Survey Professional Paper 223, 289-312

Pertlik, F. (1984a) Crystal Chemistry of Natural Tellurides 1: Redetermination of the Crystal Structure of Sylvanite. Tschermaks Mineralogische und Petrographische Mitteilungen 33, 203-212

Pertlik, F. (1984b) Crystal Chemistry of Natural Tellurides II: Redetermination of the Crystal Structure of Krennerite. Tschermaks Mineralogische und Petrographische Mitteilungen 33, 253-262

Pertlik, F. (1984c) Crystal Chemistry of Natural Tellurides III: Redetermination of the Crystal Structure of Calaverite. Zeit. Krist. 169 (1-4): 227-236

Saunders, J.A. (1986) Petrology, Mineralogy, and Geochemistry of Representative Gold Telluride Ores from Colorado. 171p. PhD thesis, Colorado School of Mines

Schutte, W.J. and De Boer, J.L. (1988) Valence Fluctuations in the Incommensurately Modulated Structure of Calaverite AuTe2. Acta Crystallographica, B44, 486-494

Sheldrick, G.M. (1997) SHELXL-97, Program for Refinement of Crystal Structures. University of Göttingen, Germany

Tunell, G. and Ksanda C.J. (1936) The crystal structure of krennerite. Washington Academy of Sciences, 26, 507-509

Tunell, G. (1941) The Atomic Arrangement of Sylvanite. The American Mineralogist, vol. 26, No. 8, 457-477

Tunell, G. and Murata K.J. (1950) The atomic arrangement and chemical composition of krennerite. The American Mineralogist, 35, 959-984

Tunell, G. (1954) The Crystal Structures of the Gold-Silver Tellurides. University of California, Los Angeles. Office of Naval Research, Contract N6 onr 275, Task Order 10, Research Project NR-081-105.